Supporting Information of

Cryogenic toughness of natural silk and a proposed structure-function relationship

Chengjie Fu,[a]‡ Yu Wang,[a]‡ Juan Guan,[b] Xin Chen,[a] Fritz Vollrath,[c] Zhengzhong Shao[a]*

[a]State Key Laboratory of Molecular Engineering of Polymers, Advanced Materials Laboratory, Department of Macromolecular Science, Fudan University, Shanghai 200433, People's Republic of China.

[b]School of Materials Science and Engineering, Beijing Innovation Center of Biomedical Engineering, Beihang University, No.37 Xue Yuan Road, Haidian District, Beijing 100191, People's Republic of China.

[c]Department of Zoology, University of Oxford, South Parks Road, Oxford OX1 3PS, United Kingdom.

‡These authors contributed equally to this work.

E-mail: zzshao@fudan.edu.cn

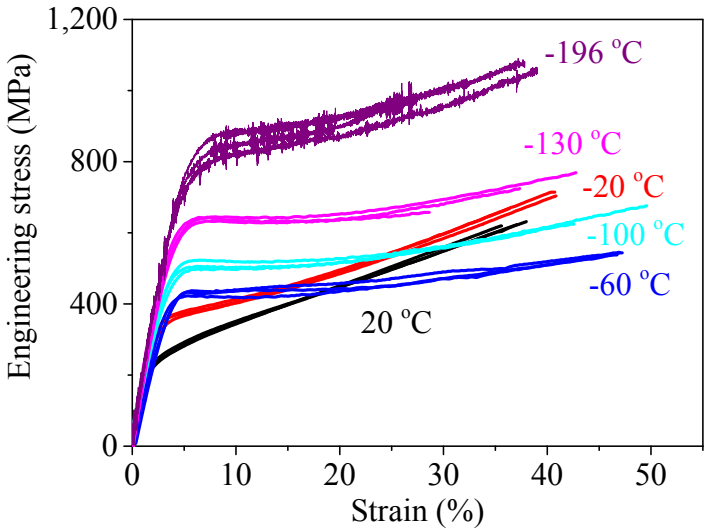

Fig. S1. Representative stress-strain curves of as-reeled *A. pernyi* silk fibers at temperatures from room temperature to liquid nitrogen temperature. Strain rate is 0.0005 s^{-1}. The data of liquid nitrogen temperature was from Instron test, others were from DMTA tests.

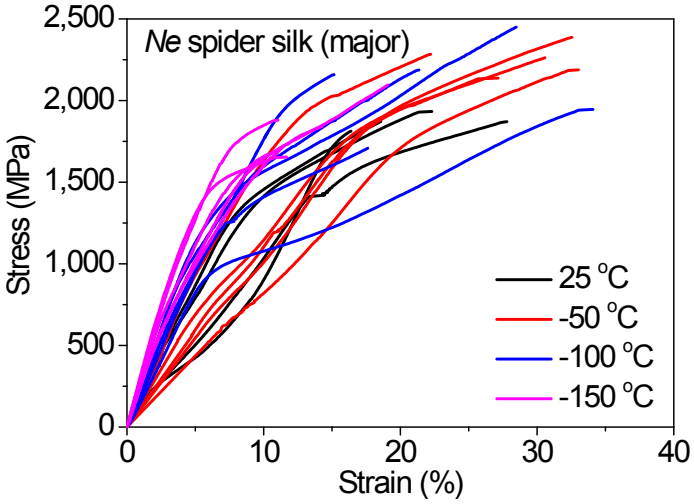

Fig. S2. Representative stress-strain curves of spider dragline silk at different temperatures. Strain rate is 0.0005 s^{-1}. The data were from DMTA tests.

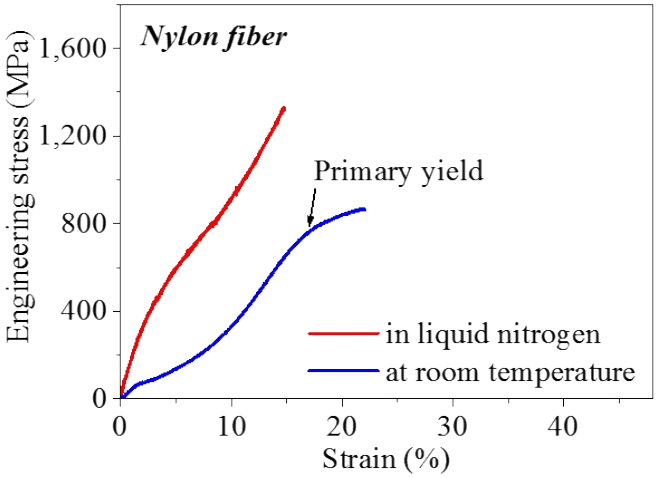

Fig. S3. Representative stress-strain curves of high tenacity nylon fibres in liquid nitrogen and in nitrogen gas at room temperature. Strain rate is 0.0005 s^{-1}.

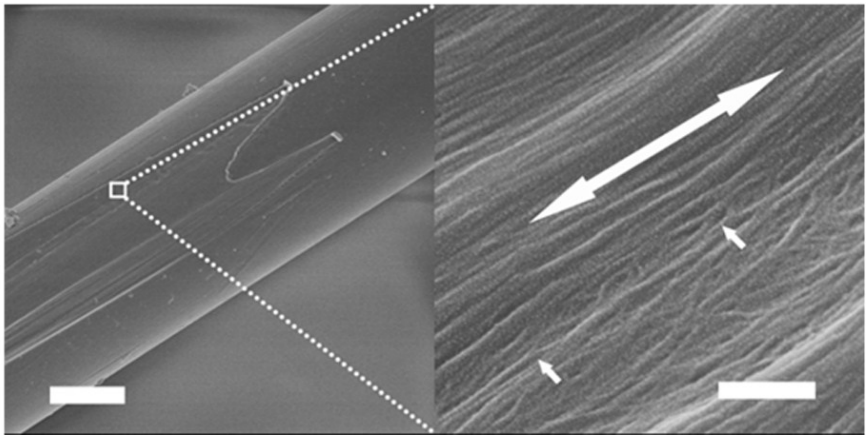

Fig. S4. Longitudinal sections of High tenacity nylon 6,6 fiber produced by peeling. The fiber rarely show microfibers during peeling. Enlarged image of the indicated rectangular area displays that the nanofilaments of a nylon fiber are merged with each other, as indicated by little white arrows. The white double-arrow indicates the long axis of the fiber. Scale bars: 10 μm (left) and 200 nm (right).

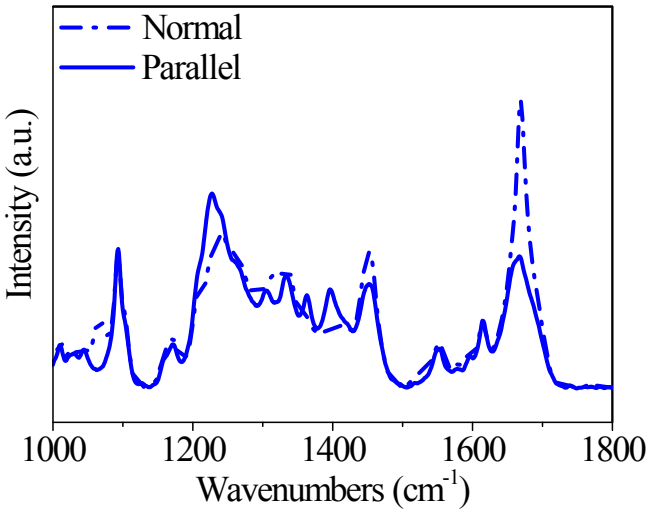

Fig. S5. Raman spectra of as-reeled *A. perny* silk fibrer collected with the fiber in the direction parallel or normal to the vibration direction of the laser light. The obvious difference between the parallel and the normal spectrum reveals that the protein chains are aligned along the fiber axis.

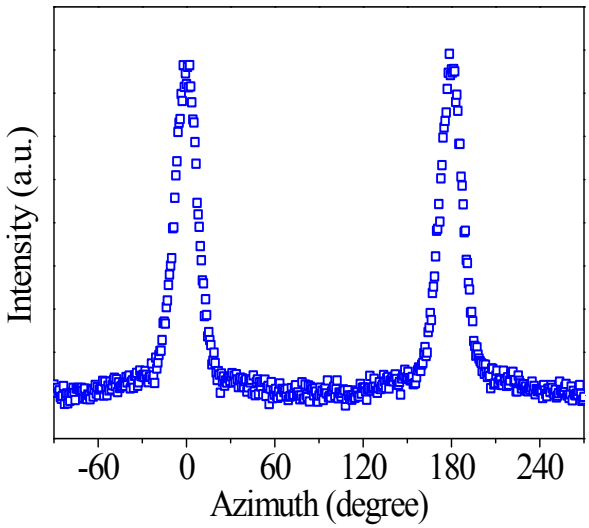

Fig. S6. XRD spectrum of commercial *A. pernyi* silk fiber measured by azimuthal scan at $2\theta = 16.8^{o}$, i.e. the diffraction from (020) planes of polyalanine β–sheet crystallites. To get a quantitative understanding of the anisotropy in *A. pernyi* silk, a Hermans orientation coefficient of 0.904 was calculated from it. Hermans orientation coefficient reveals the degree of crystalline orientation, and varies from 0 to 1, with 0 for no preferential orientation while 1 for full orientation. The large Hermans orientation coefficient of *A. pernyi* silk implies highly anisotropic structure.

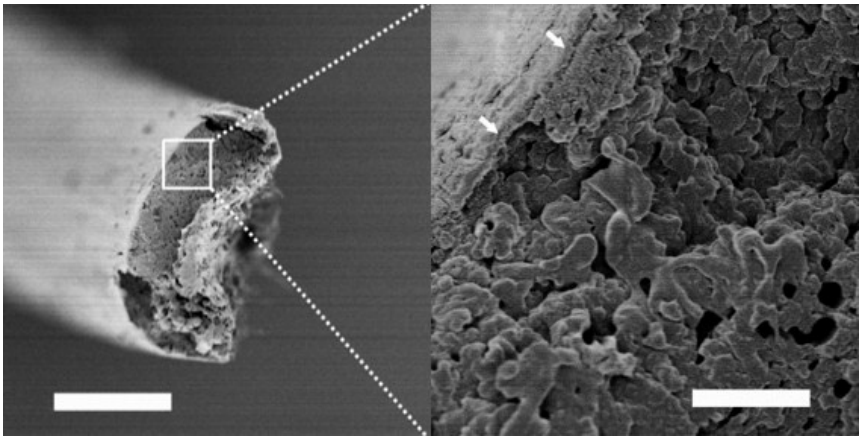

Fig. S7. Representative fractographs of degummed *A. pernyi* silk broken in liquid nitrogen. The crack initiator on the surface of the silk fibre is absent. Arrows indicate the outermost layer of the silk fibre. Scale bars: 10 μm (left) and 1 μm (right).

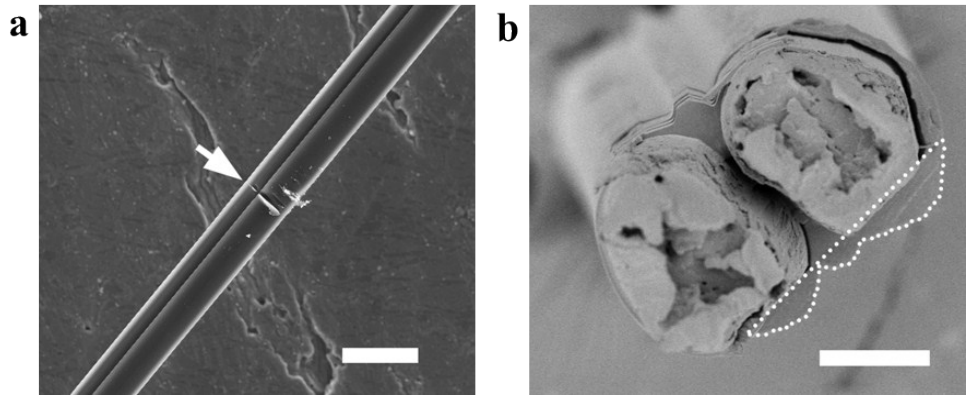

Fig. S8. Representative images of notched *A. pernyi* silk fibre. (a) Side view of the fibre with a notch indicated by the arrow. The scale bar corresponds to 50 μm. (b) Fracture end of notched *A. pernyi* silk fibre broken in semi-ductile way in liquid nitrogen. The region surrounded by the dot line is the notch. The scale bar corresponds to 10 μm

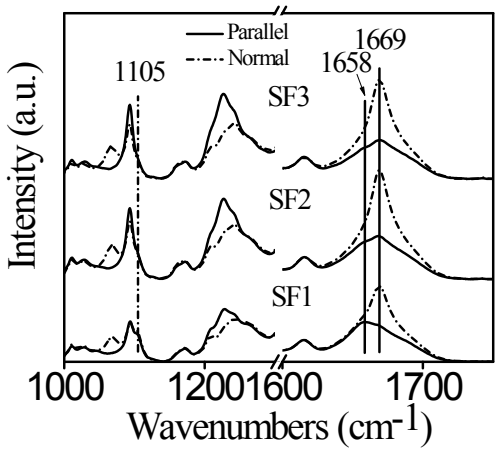

Fig. S9. Raman spectra of three representative *A. pernyi* silks. A silk fibre was aligned either parallel (solid line) or perpendicular (dashed line) to the vibration direction of the laser light.

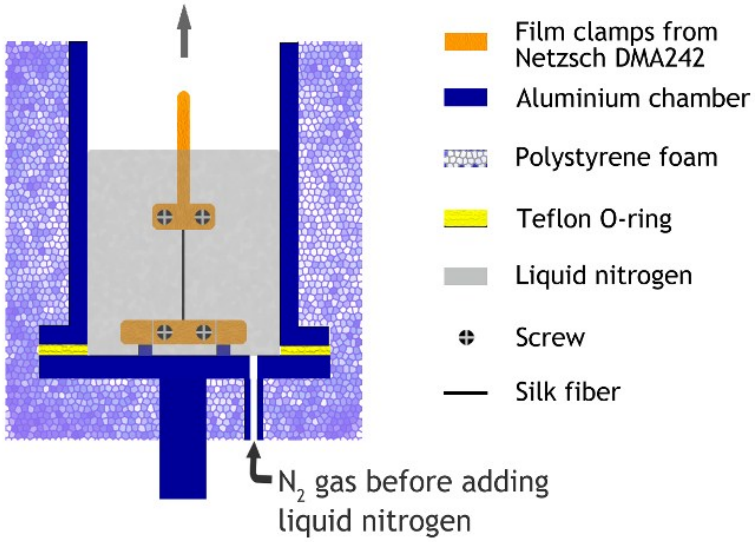

Fig. S10. Custom-built low temperature accessory for tensile test in liquid nitrogen. The aluminum chamber was fixed on the base of Instron 5565, while the upper clamp was connected to a 2.5 N load cell through a hollow aluminium beam.